Human Molecular Genetics, 2005, Vol. 14, No. 9 ***1127–1137***
doi:10.1093/hmg/ddi125
Advance Access published on March 16, 2005

Accumulation of very long-chain fatty acids does not affect mitochondrial function in adrenoleukodystrophy protein deficiency

Iris Oezen[1,†], Walter Rossmanith[2,†], Sonja Forss-Petter[1], Stephan Kemp[3], Till Voigtländer[4], Karin Moser-Thier[2], Ronald J. Wanders[3], Reginald E. Bittner[2] and Johannes Berger[1,*]

[1]Center for Brain Research and [2]Center for Anatomy and Cell Biology, Medical University Vienna, A-1090 Vienna, Austria, [3]Laboratory for Genetic Metabolic Diseases, Academic Medical Centre, University of Amsterdam, 1105 AZ Amsterdam, The Netherlands and [4]Institute of Clinical Neurology, Medical University Vienna, A-1090 Vienna, Austria

Received February 8, 2005; Revised and Accepted March 8, 2005

X-linked adrenoleukodystrophy (X-ALD, OMIM 300100) is a severe inherited neurodegenerative disease, associated with the accumulation of very long-chain fatty acids (VLCFA). The recent unexpected observation that the accumulation of VLCFA in tissues of the *Abcd1*-deficient mouse model for X-ALD is not due to a deficiency in VLCFA degradation, led to the hypothesis that mitochondrial abnormalities might contribute to X-ALD pathology. Here, we report that in spite of substantial accumulation of VLCFA in whole muscle homogenates, normal VLCFA levels were detected in mitochondria obtained by organellar fractionation. Polarographic analyses of the respiratory chain as well as enzymatic assays of isolated muscle mitochondria revealed no differences between X-ALD and control mice. Moreover, analysis by electron microscopy, revealed normal size, structure and localization of mitochondria in muscle of both groups. Similar to the results obtained in skeletal muscle, the mitochondrial enzyme activities in brain homogenates of *Abcd1*-deficient and wild-type animals also did not differ. Finally, studies on mitochondrial oxidative phosphorylation in permeabilized human skin fibroblasts of X-ALD patients and controls revealed no abnormalities. Thus, we conclude that the accumulation of VLCFA *per se* does not cause mitochondrial abnormalities and vice versa—mitochondrial abnormalities are not responsible for the accumulation of VLCFA in X-ALD mice.

INTRODUCTION

X-linked adrenoleukodystrophy (X-ALD) is an inherited neurodegenerative disease with highly variable phenotypes even among siblings. The most frequent phenotypes are the childhood cerebral X-ALD with inflammatory cerebral demyelination, and adrenomyeloneuropathy (AMN) the adult-onset, slowly progressive form that affects mainly the spinal cord and the peripheral nerves of the limbs. Both forms may occur in combination with adrenocortical insufficiency which, however, may also be the only clinical manifestation ('Addison-only' phenotype) for a long period in life (1,2).

All forms of X-ALD are caused by mutations in the *ABCD1* gene, encoding the peroxisomal 'ATP-binding cassette' (ABC) transporter, adrenoleukodystrophy protein (ALDP). ALDP-deficiency results in increased levels of saturated very long-chain fatty acids (VLCFA, >C22:0), which are normally catabolized by peroxisomal β-oxidation (2,3). The ABC transporter superfamily subgroup D includes in addition to ALDP, three other transporters that are localized in the peroxisomal membrane: ABCD2/ALD-related protein (4), the 70 kDa peroxisomal membrane protein, ABCD3/PMP70 (5) and ABCD4/PMP70-related protein (6,7) with 63, 36 and 25% amino acid identity to ALDP, respectively (7). The exact function of ALDP and the substrate it transports across

*To whom correspondence should be addressed at: Center for Brain Research, Medical University Vienna, Spitalgasse 4, A-1090 Vienna, Austria. Tel: +43 1427762812; Fax: +43 142779628; Email: johannes.berger@meduniwien.ac.at
†The authors wish it to be known that, in their opinion, the first two authors should be regarded as joint First Authors.

the peroxisomal membrane are currently unknown. However, the topology of ALDP with the ATP-binding site located towards the cytoplasm, strongly suggests that it transports a substrate from the cytoplasm into the peroxisomes.

To analyse the cellular function of ALDP, a mouse model for X-ALD was generated by targeted inactivation of *Abcd1* (8–10). VLCFA accumulate in the tissues of X-ALD mice, very similar to X-ALD patients, and cultured primary fibroblasts from *Abcd1* knockout mice show reduced rates of VLCFA β-oxidation. Older *Abcd1*-deficient mice have been described to develop a mild neurological and behavioural phenotype, starting at ∼15 months of age, with slower sciatic nerve conduction velocity and myelin and axonal abnormalities detectable in the spinal cord and sciatic nerve when compared with age-matched wild-type mice (11).

It was long assumed that the reduced ability to activate VLCFA, and thus insufficient degradation of VLCFA, well established in cultured X-ALD fibroblasts, leads to the accumulation of VLCFA in tissues (12–15). However, McGuinness *et al.* (16) recently demonstrated that the peroxisomal β-oxidation capacity is normal in tissues of Aldp-deficient mice. Moreover, mice deficient for very long-chain acyl-CoA synthetase, an enzyme that activates VLCFA for degradation in peroxisomes, have reduced peroxisomal β-oxidation but normal VLCFA levels (17). Thus, the peroxisomal β-oxidation and the accumulation of VLCFA seem to be uncoupled in ALDP-deficiency and it remains unclear how ALDP is involved in the accumulation of VLCFA. An indirect mechanism related to mitochondrial dysfunction was suggested to be responsible for the disease-characteristic accumulation of VLCFA in X-ALD (16). First, in fibroblasts from X-ALD patients, a close relationship between the rate of mitochondrial β-oxidation of VLCFA and peroxisomal β-oxidation of VLCFA was observed (16). Secondly, in fibroblasts with either mitochondrial (very-) long-chain fatty acyl-CoA dehydrogenase deficiency or carnitine palmitoyltransferase 1 deficiency, the significantly reduced mitochondrial LCFA β-oxidation is accompanied by a significant reduction of peroxisomal VLCFA β-oxidation, implying interdependence of the two processes. Therefore, it has been postulated that ALDP-deficiency influences mitochondrial function causing an increase in the level of LCFA in the cell and, because peroxisomal very long-chain acyl-CoA synthetase has a higher affinity for LCFA than for VLCFA (18), the net effect would be a backlog of VLCFA in the cytoplasm. In addition, it was suggested that mitochondrial abnormalities might lead to increased fatty acyl chain elongation and thus to the accumulation of VLCFA.

In peroxisome biogenesis disorders, which are characterised by the absence or a strong reduction in the number of functional peroxisomes due to mutations or deletions in the *peroxin* (*PEX*) genes (19,20), the molecular defects manifest in the accumulation of VLCFA and phytanic acid in plasma and tissues and in the reduction of plasmalogens in erythrocytes and tissues (2). The *Pex5* (−/−) mouse, a model for Zellweger syndrome lacks functional peroxisomes and shows the severe pathological and biochemical defects seen in the Zellweger patients (21). Strikingly, these mice show, in addition to the loss of peroxisomes, mitochondrial alterations in hepatocytes (22). The mitochondria show a very heterogeneous morphology and the ultrastructural abnormalities affect all subcompartments. Ultrastructural changes were also seen in other lipid-metabolizing tissues, like adrenal cortex, kidney cells of the proximal tubules, cardiomyocytes, skeletal muscle and most prominently in the diaphragm (22). In the liver of newborn *Pex5* (−/−) mice, a decrease in complex I and V activities of the mitochondrial electron transporter chain was demonstrated (22).

Mitochondria house numerous crucial biochemical pathways and are, in particular, responsible for the generation of ATP by oxidative phosphorylation and for the β-oxidation of short-, medium- and long-chain fatty acids. To test the hypothesis that mitochondrial impairment is the cause of VLCFA accumulation or, if the accumulation of VLCFA itself could cause mitochondrial damage in X-ALD, we here assessed mitochondrial functions and morphology in the skeletal muscle of *Abcd1*-deficient mice. We carried out a detailed analysis of the mitochondrial respiratory chain using high-resolution respirometry and enzymatic assays, investigations of the peroxisomal and mitochondrial β-oxidation systems and electron microscopy with morphometric analysis in isolated mitochondria of *Abcd1*-deficient mice. In a second approach, the function of the individual respiratory chain complexes were analysed spectrophotometrically. Finally, to establish whether the mitochondrial respiratory chain function is impaired in X-ALD patients, measurements of ATP-synthesis and the formation of lactate and pyruvate from glucose in human skin fibroblasts from X-ALD patients were compared with healthy controls.

RESULTS

Accumulation of VLCFA in skeletal muscle of *Abcd1*-deficient mice

It has been shown previously that VLCFA levels are increased in fibroblasts and various tissues from X-ALD patients and Aldp-deficient mice (8–10). This analysis was now extended to include skeletal muscle tissue. For this purpose, pools were made containing the quadriceps, gastrocnemius, soleus and adductor muscles from the hind limbs of 9-month-old *Abcd1*-deficient mice and their wild-type littermates. The results from gas chromatographic analysis of total lipids demonstrated a 4-fold increase in the C26:0/C22:0 ratio in muscle tissue of *Abcd1*-deficient mice, which is comparable to the increased C26:0/C22:0 ratios found in brain, kidney and adrenals (Fig. 1).

Peroxisomal β-oxidation is normal in skeletal muscle of *Abcd1*-deficient mice

On the basis of the intriguing observation by McGuinness *et al.* (16), that peroxisomal β-oxidation of C24:0 is normal in brain, adrenals, heart, liver and kidney of *Abcd1*-deficient mice, we determined the VLCFA β-oxidation rate in a peroxisome-enriched fraction from skeletal muscle of wild-type and *Abcd1*-deficient mice and compared these with results obtained from mouse fibroblasts. In agreement with our previously published results (8), the rate of β-oxidation of lignoceric acid (C24:0) in *Abcd1*-deficient mouse fibroblasts

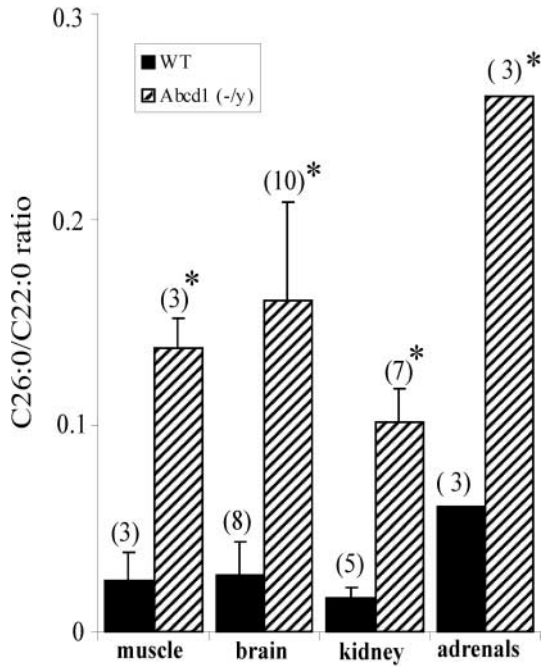

Figure 1. Accumulation of VLCFA in skeletal muscle of *Abcd1*-deficient mice. Gas chromatographic analysis of total lipids extracted from *Abcd1*-deficient and wild-type mice. The results from skeletal muscle, brain, kidney and adrenals are shown as the ratio of the concentrations obtained for C26:0 and C22:0. The number of animals analysed is indicated in parenthesis; adrenal glands were analysed as a pool of tissues from three mice. An asterisk indicates statistical significance ($P < 0.05$).

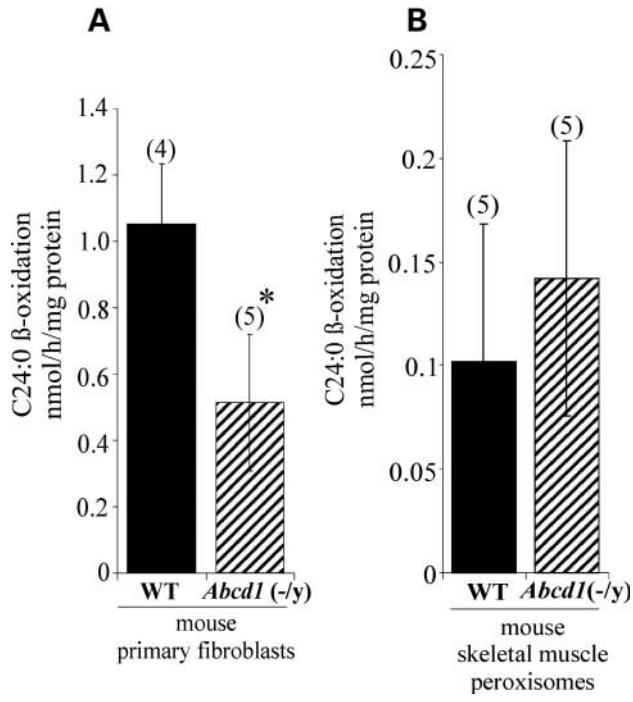

Figure 2. VLCFA β-oxidation in *Abcd1*-deficient and wild-type mouse primary fibroblasts and skeletal muscle tissue. The rate of β-oxidation of lignoceric acid (C24:0) was determined (**A**) in primary mouse fibroblasts and (**B**) mouse skeletal muscle of *Abcd1*-deficient and wild-type animals. The results are shown as mean ± standard deviation with the number of animals analysed in parenthesis. Statistically significant differences are indicated with an asterisk ($P < 0.05$). VLCFA (C24:0) β-oxidation rates are expressed as nmol/h/mg protein. Most of the catalase activity was detected in the peroxisomal fraction (data not shown), indicating that the peroxisomes are intact.

was ~50% of that in wild-type cells (Fig. 2A). Analysis of a peroxisome-enriched fraction from freshly isolated skeletal muscle, however, showed no statistically significant difference in the rate of VLCFA oxidation between wild-type and *Abcd1* knockout animals (Fig. 2B). Thus, VLCFA accumulate in skeletal muscle of Aldp-deficient mice in spite of normal peroxisomal VLCFA degradation. These results prompted us to perform a detailed analysis of mitochondrial functions.

Respiratory function of isolated mitochondria is normal in *Abcd1*-deficient mice

One of the key functions of mitochondria is the generation of ATP by oxidative phosphorylation. Therefore, we evaluated the respiratory capacity of isolated muscle mitochondria from *Abcd1*-deficient and wild-type animals by multiple substrate-inhibitor titration respirometry (Fig. 3A and B). Respiration was stimulated by oxidation of the NADH-dependent substrates pyruvate/malate or glutamate/malate (respiration through complexes I, III and IV); inhibition with antimycin A, ascorbate/tetramethyl-*p*-phenylendiamine dihydrochloride (TMPD) was used to test for respiration through complex IV only. Regardless, if respiratory activity was normalized to citrate synthase (CS) activity (Fig. 3C) or mitochondrial protein content (data not shown), no significant differences were found between *Abcd1* (−/y) and wild-type animals concerning their oxygen consumption rates on different substrates.

To assess any limitation of respiration by the phosphorylating system (complex V), ascorbate/TMPD-dependent respiration was uncoupled by the addition of carbonylcyanide-*p*-trifluoromethoxy-phenylhydrazone (FCCP). Neither in *Abcd1*-deficient nor in wild-type mitochondria did the respiratory rates increase after uncoupling (data not shown), indicating full complex V function. Moreover, respiration from both, *Abcd1*-deficient and wild-type mitochondria, was well coupled to phosphorylation as indicated by their respiratory control indices (ratio of pyruvate/malate-dependent respiration in the presence of ATP and after inhibition of the ATP–ADP translocase by atractyloside) (Fig. 3D). Mitochondrial function was also assessed by different enzymatic assays to reveal even subtle differences in respiratory chain function: NADH:O_2 oxidoreductase (representing the activity of complex I, III and IV), succinate:cytochrome *c* oxidoreductase (complex II and III), cytochrome *c* oxidase (complex IV) and CS (the mitochondrial marker enzyme). The specific CS activity of either crude muscle homogenates (data not shown) or isolated mitochondria was comparable in *Abcd1*-deficient and wild-type mice (Fig. 4A). In agreement with the mitochondrial respirometry results, also the respiratory chain specific enzymatic assays revealed no statistically significant differences (Fig. 4B–D). Taking all the results together from these thorough analyses, it has to be concluded

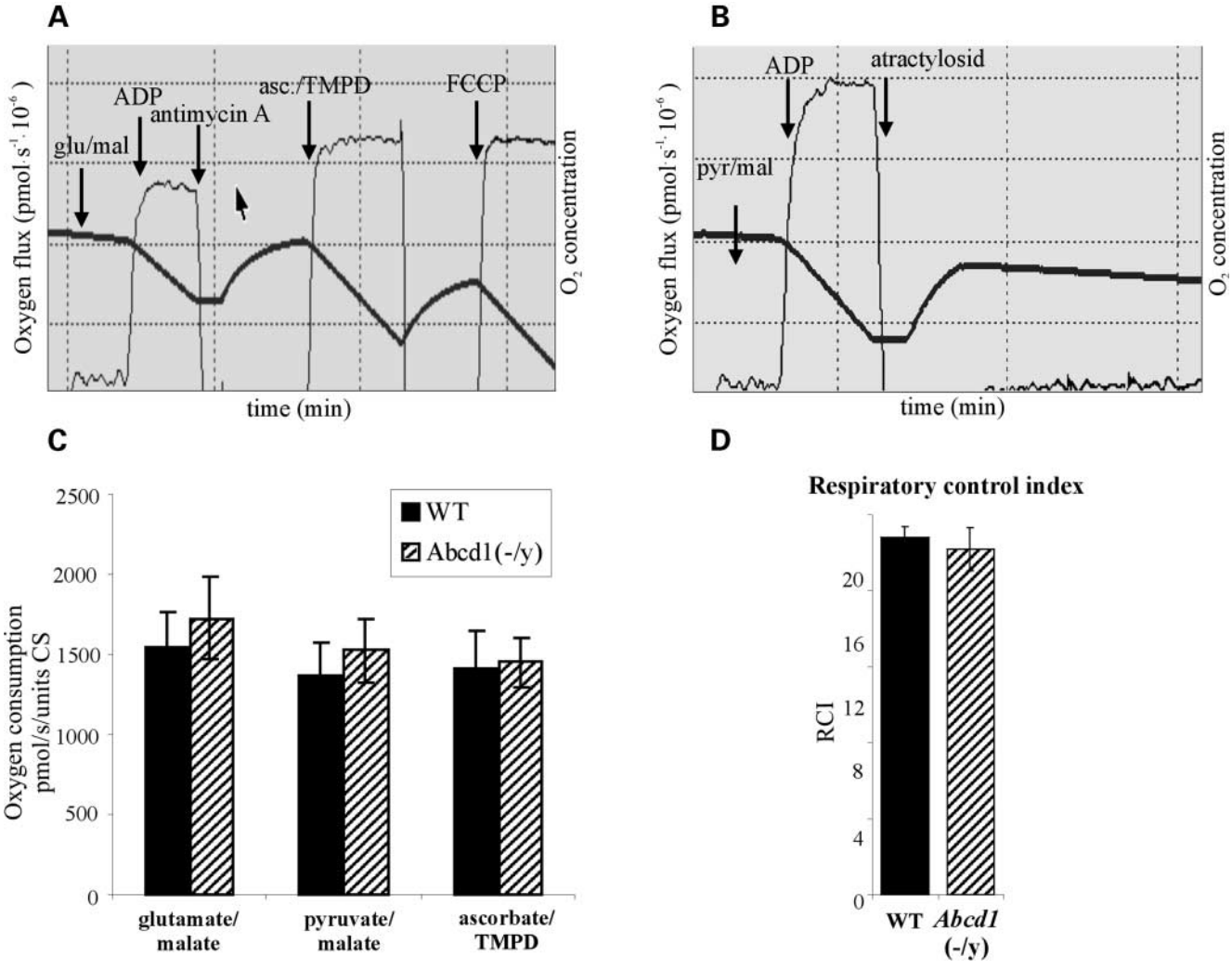

Figure 3. Respiration of isolated mitochondria from skeletal muscle of *Abcd1*-deficient and wild-type mice. (**A** and **B**) Representative oxygen concentration (thick line) and oxygen consumption rate (thin line) derived from a multiple-substrate-inhibitor analysis of isolated skeletal muscle mitochondria from *Abcd1*-deficient mice. Addition of the various substrates and inhibitors is indicated. After addition of the inhibitor antimycin A and ascorbat/TMPD in panel (A) and atractyloside in panel (B), the chamber was re-oxygenated to derive oxygen consumption rates at comparable O_2 concentrations. (**C**) Specific oxygen consumption rate on different substrates. Rates were normalized to citrate synthase activity (CS) of each sample. (**D**) Respiratory control indices (ratio of pyruvate/malate dependent respiration in the presence of ATP and after inhibition of the ATP–ADP translocase by atractyloside). The results in (A and D) are shown as mean ± standard deviation of five animals, each analysed in triplicate.

that mitochondrial respiratory function of *Abcd1*-deficient mice is not significantly altered.

Mitochondrial enzyme activities are not affected in brain of *Abcd1*-deficient mice

Because an increased level of saturated unbranched VLCFA, particularly in the cholesterol ester, ganglioside and proteolipid fractions of the brain white matter, is one major characteristic in X-ALD, we also investigated the enzymatic activities of key respiratory enzymes (NADH:O_2 oxidoreductase, succinate:cytochrome *c* oxidoreductase, cytochrome *c* oxidoreductase) and of CS from crude brain homogenates (Fig. 5). As in isolated muscle mitochondria (Fig. 4), the enzyme activities in brain of *Abcd1*-deficient mice were comparable to the levels of wild-type littermates.

LCFA β-oxidation is normal in mitochondria isolated from skeletal muscle of *Abcd1*-deficient mice

Prompted by the apparent absence of any defects in the oxidative phosphorylation system, we evaluated the mitochondrial β-oxidation using two different approaches. First, the rate of mitochondrial LCFA acid β-oxidation was assessed indirectly, using saponin-permeabilized soleus muscle fibres in high-resolution respirometry. Here, palmitoyl carnitine was used as a substrate to feed the respiratory chain via mitochondrial β-oxidation and the resulting respiratory activity was recorded. Again, no significant difference was observed between *Abcd1*-deficient and wild-type mice (Fig. 6A). Secondly, LCFA β-oxidation was measured using radioactively labelled [1-^{14}C]palmitic acid (C16:0) as a substrate for the same mitochondrial preparations as used for

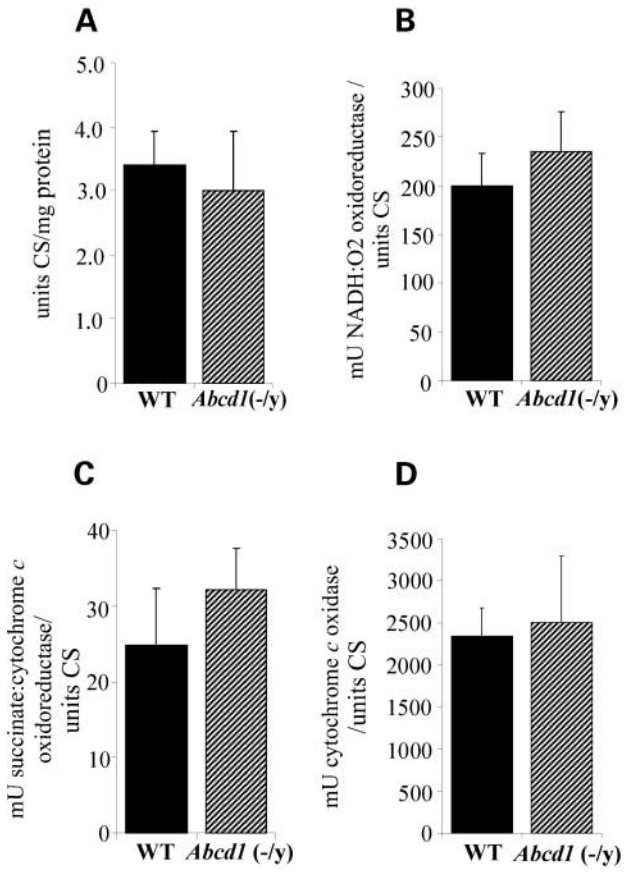

Figure 4. Mitochondrial enzyme activities in isolated muscle mitochondria of *Abcd1*-deficient and wild-type animals. **(A–D)** Activities of the mitochondrial marker CS (A) and different respiratory chain enzymes (B–D) were determined in isolated muscle mitochondria of *Abcd1*-deficient and wild-type mice. Mean respiratory chain enzymatic activities [NADH:O_2 oxidoreductase (B), succinate:cytochrome *c* oxidoreductase (C) and cytochrome *c* oxidase (D)] ± standard deviation of five animals/group normalized to CS are shown.

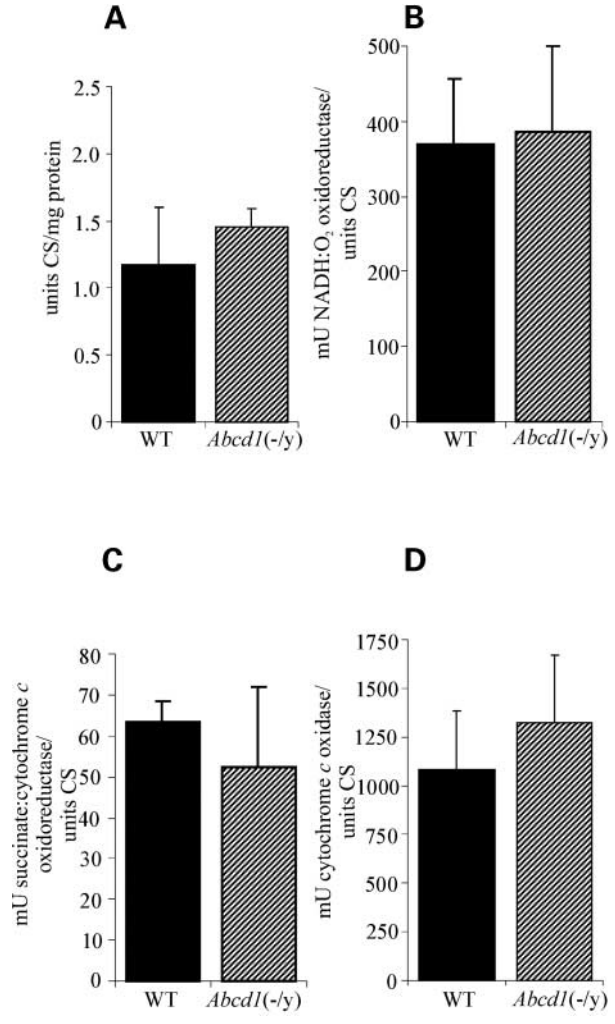

Figure 5. Mitochondrial enzyme activities in crude brain homogenates of *Abcd1*-deficient and wild-type animals. (**A–D**) The activities of the mitochondrial marker enzyme CS (A) and three mitochondrial respiratory chain enzymes: NADH:O_2 oxidoreductase (B), succinate:cytochrome *c* oxidoreductase (C) and cytochrome *c* oxidase (D) were analysed spectrophotometrically in brain homogenates of *Abcd1*-deficient and wild-type animals (three animals/group). Respiratory chain enzyme activities are shown as mean activities ± standard deviation, normalized to CS.

respirometric analyses (Fig. 6B). The ability to degrade palmitic acid was unchanged in mitochondria from X-ALD mice compared to wild-type littermates. Thus, both assays indicate unaltered mitochondrial β-oxidation capacity.

Normal ultrastructural morphology of muscle mitochondria in *Abcd1*-deficient mice

Severe ultrastructural alterations of mitochondria have been reported in the diaphragm in the Zellweger mouse model (22). Therefore, we analysed shape, size and morphology of mitochondria in the diaphragm from two 12-month-old *Abcd1* knockout mice and three male wild-type littermates by electron microscopy. Ultrastructural inspection of mitochondria in the diaphragm of *Abcd1*-deficient mice revealed no alterations in number, structure or localization compared with their wild-type littermates (Fig. 7A and B). In addition, morphometric analysis of the perimeter of several hundred mitochondria from each genotype indicated a similar size of mitochondria in both groups (Fig. 7C). Taken together, these results were in line with the normal activities observed for CS and the respiratory chain enzymes.

The mitochondrial membranes of *Abcd1*-deficient mice do not accumulate VLCFA

As the mitochondrial membrane contains a substantial amount of phosphatidylcholine, a phospholipid known to contain a high amount of VLCFA in X-ALD (23), we determined the VLCFA content of isolated mitochondria from gastrocnemius muscle of wild-type and *Abcd1*-deficient mice (Fig. 8). No accumulation was found in the mitochondrial fraction from X-ALD mice, in spite of the robust increase in VLCFA in whole skeletal muscle homogenate (Fig. 1).

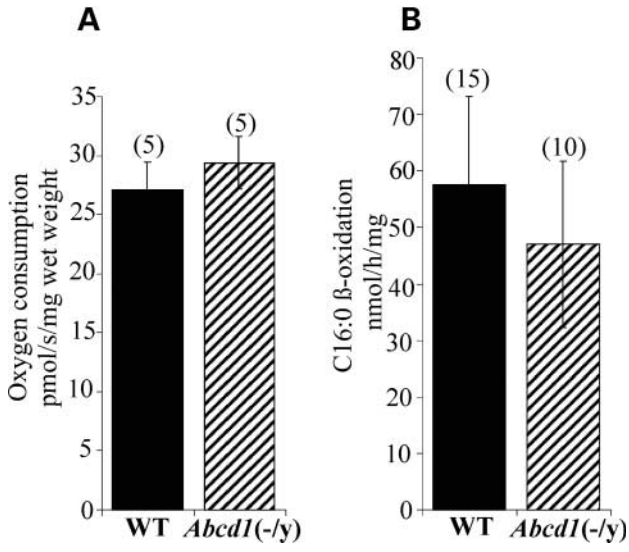

Figure 6. Mitochondrial β-oxidation of *Abcd1*-deficient and wild-type animals. (**A**) Palmitoyl carnitine dependent respiration of permeabilized muscle fibres. Mean ± standard deviation of the respiratory rates per milligram muscle fibre wet weight of five animals, each analysed in quadruplicate, are shown. (**B**) The rate of β-oxidation of palmitic acid ($C_{16:0}$) was measured in mitochondria isolated from skeletal muscle of *Abcd1*-deficient and wild-type mice. The specific activity is shown as mean ± standard deviation with the number of animals analysed indicated in parenthesis.

Measurement of ATP-synthesis and the formation of lactate and pyruvate from glucose in human skin fibroblasts

To establish whether the mitochondrial respiratory chain function is impaired in X-ALD patients, we measured ATP-synthesis with glutamate/malate and succinate/rotenone and the formation of lactate and pyruvate from glucose in primary human fibroblasts from X-ALD patients and compared these results with data obtained in healthy controls and cells from patients with cytochrome *c* oxidase deficiency (Table 1). No difference in both, ATP-synthesis and the lactate to pyruvate ratio, were observed between X-ALD and control fibroblasts. For comparison, the severely decreased rate of ATP production in fibroblast cell lines from two patients with cytochrome *c* oxidase deficiency are shown, representing values typical for an impairment of the respiratory chain-driven ATP-synthesis (24). In addition, the effect of sodium azide (inhibitor of cytochrome *c* oxidase) treatment on the lactate and pyruvate production in normal fibroblasts was included to demonstrate the strong increase in the lactate to pyruvate ratio that would have been expected, if the mitochondrial oxidative phosphorylation were defective in X-ALD (25).

DISCUSSION

The unexpected observation that X-ALD mouse tissues have normal levels of peroxisomal VLCFA β-oxidation in the absence of Aldp and yet have elevated VLCFA levels, with the consequential hypothesis that mitochondria are involved in the X-ALD pathology (16), prompted us to look closer at the mitochondrial functions in X-ALD. Elevated levels of

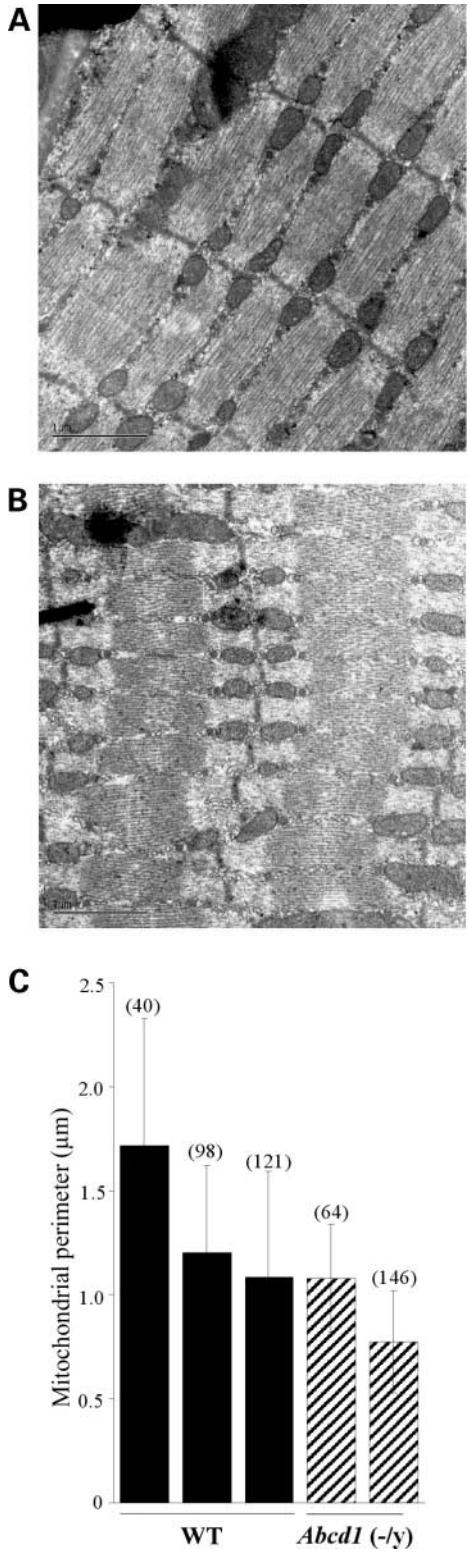

Figure 7. Ultrastructural analysis of mitochondria from diaphragm of *Abcd1*-deficient and wild-type mice. The diaphragm of (**A**) a 12-month-old *Abcd1*-deficient and (**B**) a wild-type mouse was analysed by electron microscopy. The perimeter of the indicated number of mitochondria from three wild-type and two Abcd1-deficient mice was determined morphometrically (**C**). The values between the two groups show no statistically significant difference according to Student's *t*-test.

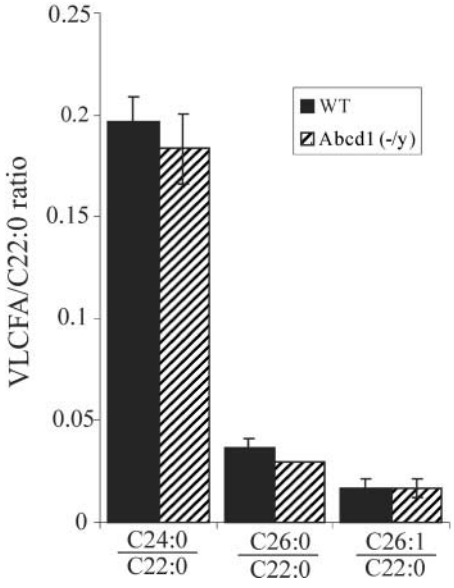

Figure 8. Analysis of VLCFA levels in isolated mitochondria from skeletal muscle of *Abcd1*-deficient and wild-type mice. VLCFA levels in 100 μg of isolated mitochondria were determined by electrospray ionization mass spectrometry. The results are indicated as ratios of C24:0/C22:0, C26:0/C22:0 and C26:1/C22:0.

VLCFA are a major diagnostic feature of X-ALD and other peroxisomal disorders (26–28). First, we established that the loss of Aldp results in substantial accumulation of VLCFA (C26:0) and also in murine skeletal muscle. Two main reasons motivated us to choose muscle tissue for a detailed analysis of mitochondrial functions in X-ALD. Already in 1979, characteristic biochemical and ultrastructural abnormalities in cultured muscle cells from a patient with AMN were reported (29). Another reason was that mitochondrial defects are usually well reflected in muscle tissue and, therefore, we expected to obtain clear results from this study.

In contrast to human X-ALD patients, plasma VLCFA levels are not increased in *Abcd1*-deficient mice. Thus, the accumulation of VLCFA in muscle is not due to uptake of VLCFA from the blood but rather caused by a metabolic deficiency in the muscle cell itself. Although *Abcd1*-deficient muscle tissue displayed clearly elevated concentrations of VLCFA (C26:0) and a C26:0/C22:0 ratio comparable to those in brain, kidney and adrenals, it was surprising that isolated mitochondria from skeletal muscle of these mice did not show an increased VLCFA content. Moreover, in good agreement with recently published results (16), we found near normal levels of peroxisomal VLCFA β-oxidation in muscle tissue from *Abcd1*-deficient mice despite the elevated levels of VLCFA.

In fibroblasts, it has been shown that the rate of peroxisomal β-oxidation is dependent on the rate of mitochondrial β-oxidation, as fibroblasts deficient in mitochondrial long-chain fatty acyl-CoA dehydrogenase or carnitine palmitoyltransferase 1 show reduced LCFA as well as VLCFA β-oxidation activity (16). In contrast, tissues from *Abcd1*-deficient mice do not show impaired peroxisomal β-oxidation rates. Analyses

Table 1. Measurement of ATP-synthesis and the formation of lactate and pyruvate from glucose in human skin fibroblasts

	ATP-synthesis[1]	Lactate:pyruvate ratio
Controls ($n = 105$)	18.8 ± 4.0	19.2 ± 7.1
X-ALD ($n = 7$)	15.2 ± 7.1	15.1 ± 6.6
Controls + azide ($n = 105$)	n.d.	78.4 ± 22.4
Cytochrome *c* oxidase deficiency ($n = 2$)	1.02; 1.13	n.d.

Results are shown as mean ± standard deviation. n.d., not determined.
[1]ATP-synthesis expressed as nmol/min/mg protein.

of the *Pex5*-deficient mouse model of Zellweger syndrome have shown that defective peroxisome biogenesis is associated with mitochondrial alterations leading to mitochondrial respiratory chain dysfunction and to diverse cellular responses (21). Mitochondrial pathology has also been described in human Zellweger patients (30). However, our analysis of primary fibroblasts from X-ALD patients did not demonstrate impaired mitochondrial function, as measured by either ATP-synthesis rate or the lactate to pyruvate ratio (Table 1).

At the biochemical level, several different approaches are available to determine mitochondrial respiratory chain dysfunctions. The activity of respiratory chain complexes may be analysed spectrophotometrically by measuring different enzymatic activities or, alternatively, they may be examined in intact organelles by multiple substrate-inhibitor titration respirometry (31,32). The study of mitochondrial respiratory parameters provides an important tool to understand mitochondrial physiology and the potential role of mitochondria in pathology. To answer the question whether mitochondrial defects could contribute to the pathology of X-ALD, we first analysed specific respiratory functions in *Abcd1*-deficient mice and their wild-type littermates by applying high-resolution respirometry to isolated mitochondria from skeletal muscle. Our results conclusively demonstrated normal respiratory chain function in *Abcd1*-deficient mice (Fig. 3C). No substrate dependent differences in respiratory chain activity could be observed between X-ALD and wild-type animals in skeletal muscle. Spectrophotometric measurements of isolated muscle mitochondria confirmed the polarographic data and thus provided complementary information about the function of the individual respiratory chain complexes in skeletal muscle of Abcd1-deficient mice and wild-type animals.

We extended the spectrophotometric analysis on murine brain homogenates to exclude potential respiratory deficiencies. When compared with the wild-type control group, no changes in the activity of respiratory enzymes were observed in *Abcd1*-deficient mice (Fig. 5). Brain has been chosen as a second study-tissue, because it is more strongly affected by X-ALD pathology than skeletal muscle, yet similarly to muscle it is typically severely affected by mitochondrial dysfunctions. Normal enzyme activity in brain homogenates does not exclude subtle mitochondrial dysfunction, as tissues have different thresholds of tolerance to mitochondrial dysfunction. Brain relies primarily on oxidative phosphorylation and its threshold of tolerance should be rather low. In another approach, saponin-permeabilized muscle fibres from soleus muscle of *Abcd1*-deficient mice

were investigated by high-resolution respirometry. Mitochondria in intact muscle fibres are organized within the surrounding cytoskeletal network and are integrated into functional clusters. It is assumed that these clusters are connected to each other and are so able to respond in a synchronized fashion to physiological changes. With the substrate palmitoyl carnitine, we were able to assess respiratory chain function driven by mitochondrial β-oxidation. Again, no significant differences between knockout and wild-type mice were observed. These results were consistent with normal LCFA (C16:0) β-oxidation rates in mitochondria isolated from muscle tissue of *Abcd1*-deficient mice (Fig. 6B). Both results demonstrate that animals lacking Aldp show neither impaired mitochondrial β-oxidation nor reduced activity of the respiratory chain.

Pharmacologically induced expression of the ALD-related (ALDR/ABCD2) protein or overexpression of transfected ALDR cDNA can correct peroxisomal VLCFA β-oxidation in primary human fibroblasts derived from X-ALD patients (33). When Aldr cDNA is overexpressed as a transgene in *Abcd1*-deficient mice, tissue levels of VLCFA normalise. In normal murine skeletal muscle, both *Abcd1* and *Abcd2* are expressed at relatively high levels (34). To exclude the possibility that Aldr protein compensates for *Abcd1*-deficiency in muscle and therefore abrogates mitochondrial dysfunction, we also subjected *Abcd2*-deficient and *Abcd1*/*Abcd2*-double deficient mice to the same analysis. However, for both single knockout and the double knockout groups, all results indicated normal mitochondrial functions (manuscript in preparation).

To further rule out any mitochondrial defects, the ultrastructure, localization and size of mitochondria were determined. In *Pex5*, the absence of functional peroxisomes leads to mitochondrial alterations in different tissues and blood cells (22). These mice exhibit severe alterations in the diaphragm, varying from small blebs with electron lucent content in the outer membrane to morphological changes in the cristae structure-like arrangements into parallel stacks or curvilinear and circular forms. Mitochondria of the diaphragm were more severely affected than those of the skeletal muscle (21,22). We also investigated the diaphragm of *Abcd1* mice by electron microscopy. The electron micrographs revealed normal distribution and localization of the mitochondria along the Z-fibres in the muscle fibre, and by morphometric analysis the size of the mitochondria was unaltered. Thus, in contrast to the mitochondrial abnormalities in Zellweger syndrome, *Abcd1*-deficient mice do not show ultrastructural modification in size, structure or localization of mitochondria in the diaphragm.

Patients with Refsum disease, a peroxisomal disorder associated with α-oxidation deficiency, demonstrate that the accumulation of phytanic acid at high levels throughout the body. Phytanic acid is incorporated into the mitochondrial membranes, increases the membrane H^+ conductance and disturbs protein-linked functions in energy coupling. The reduction in mitochondrial ATP supply and opening of the permeability transition pore are two major mechanisms that induce the onset of the degenerative process (35). In contrast, our results indicate that VLCFA are not incorporated into mitochondrial membranes of skeletal muscle although these consist to about 45% of phosphatidylcholine. Hexacosanoic acid (C26:0) is known to accumulate in glycerophospholipds, in particular phosphatidylcholine, of X-ALD white matter (23). On the basis of this observation, we would have expected VLCFA accumulation in the membranes of the skeletal muscle mitochondria of *Abcd1*-deficient mice. However, a normal fatty acid composition of mitochondrial membranes (Fig. 8) was determined. This finding is consistent with the unimpaired respiratory control (Fig. 3D), indicating tight coupling between respiration and phosphorylation, as well as correct membrane function with respect to proton leakage. Thus, excessive VLCFA are apparently neither incorporated into mitochondrial membranes nor do they disturb mitochondrial respiratory chain function and ATP synthesis.

We conclude that the accumulation of VLCFA *per se* does not cause mitochondrial abnormalities and vice versa, our results imply that mitochondrial abnormalities are not the origin of the accumulation of VLCFA in X-ALD, even though we cannot rule out that *Abcd1*-deficiency might lead to more subtle mitochondrial dysfunction. Furthermore, it cannot be excluded that *Abcd1*-deficiency contributes to mitochondrial impairment in other tissues, where mitochondria are highly involved in more specialised functions, like steroid production in adrenocortical cells.

Because peroxisomal β-oxidation in *Abcd1*-deficient muscle tissue is normal as was shown for several other tissues (including brain) (16), the increased VLCFA levels in X-ALD do not seem to result from reduced β-oxidation activity but rather from increased elongation of LCFA and VLCFA and/or modified incorporation of VLCFA in complex lipids. This hypothesis is supported by the finding that even in fibroblasts from X-ALD patients, where peroxisomal β-oxidation is impaired, Kemp *et al.* (36) demonstrated an enhanced VLCFA elongation, which could account for the accumulation of VLCFA in X-ALD.

Taken together, mitochondrial defects do not seem to be a primary defect in X-ALD. However, it cannot be excluded that secondary mitochondrial dysfunction occurs in affected tissues such as the degenerating central nervous system.

MATERIALS AND METHODS

Unless otherwise specified, chemicals were purchased from Sigma-Aldrich (St Louis, MO, USA).

Animals

Male *Abcd1*-deficient mice (8) obtained after 10 generations of backcrossing to the inbred C57BL/6 strain and their wild-type littermates were used for experimental analyses at an age of 12–16 months, as indicated. The mice were housed at 22°C, on a 12 h light/dark cycle, with free access to food and water. Procedures involving animals were conducted in conformity with the institutional guidelines that are in compliance with national and international laws and policies. All subsequent analyses were performed in a blinded fashion with respect to the genotype of the mice.

Preparation of crude tissue homogenates for assays of mitochondrial enzyme activities

Gastrocnemius muscle and brain were dissected and immediately snap frozen in liquid nitrogen. All steps were performed at 4°C, if not stated otherwise. Approximately 20 mg of frozen muscle tissue and half a frozen brain (200 mg) were homogenized in a Teflon-glass Potter-Elvehjem homogenizer in 20 volumes (ml/g of tissue) SETH buffer (250 mM sucrose, 2 mM EDTA, 10 mM Tris–Cl, pH 7.4, 50 U Heparin/ml) for 1.5 min and centrifuged at 600*g* for 15 min. 100 µl of a 1:10 dilution of these preparations were used for CS activity measurements. For the determination of the enzyme activities in the brain homogenate, 30 µl for NADH:O_2 oxidoreductase, 40 µl of a 1:2 dilution for succinate:cytochrome *c* oxidoreductase and 40 µl of a 1:20 dilution for cytochrome *c* oxidase were used.

Isolation and preparation of muscle mitochondria

Muscles were dissected freshly from 14-month-old wild-type and *Abcd1* (−/y) male littermates. Skeletal muscle mitochondria were isolated from 1–2 g of hindlimb skeletal muscles including gastrocnemius, adductors and quadriceps muscles. For the isolation procedure, all steps were carried out on ice or at 4°C. The muscle tissue was freed from collagen, nerves and fat, minced, weighed and homogenized in a Teflon-glass Potter-Elvehjem homogenizer in 10 ml isolation buffer (220 mM mannitol, 70 mM sucrose, 1 mM EDTA, 10 mM Tris–Cl, pH 7.5) per gram of tissue. After centrifugation at 1000*g* for 5 min, the supernatant was collected. This step was repeated twice to remove tissue debris. Finally, mitochondria were collected by centrifugation at 8000*g* for 15 min, washed once with isolation buffer, re-pelleted and resuspended in isolation buffer (100 µl/g initial material). After the use for polarographic studies, the isolated mitochondria were frozen in liquid nitrogen and stored at −80°C for later spectrophotometric measurements. For the determination of the enzyme activities of the isolated mitochondria, 100 µl of a 1:100 dilution for CS determination, 30 µl of a 1:50 dilution for NADH:O_2 oxidoreductase, 40 µl of a 1:50 dilution for succinate:cytochrome *c* oxidoreductase and 40 µl of a 1:100 dilution for cytochrome *c* oxidase were used. CS activity was determined with 100 µl of a 1:100 dilution of permeabilized mitochondria.

Preparation of soleus muscle for polarographic measurements

Freshly dissected soleus muscle was immediately transferred into ice-cold BIOPS buffer pH 7.1 (2.77 mM CaK_2EGTA, 7.23 mM K_2EGTA, 5.7 mM Na_2ATP, 5.56 mM $MgCl_2$, 20 mM taurine, 15 mM Na_2-phospho-creatinine, 20 mM imidazole, 0.5 mM dithiothreitol, 50 mM MES). The fibres were cut in half, loosened with forceps under a binocular microscope and incubated for 30 min in BIOPS buffer with 50 µg/ml saponin at 4°C. The fibre bundles were washed for 10 min at 4°C in respiration buffer 2 [0.5 mM EGTA, 3 mM $MgCl_2$, 60 mM K-lactobionate, 20 mM taurine, 10 mM KH_2PO_4, 20 mM HEPES, 110 mM sucrose, 0.1% (w/v) bovine serum albumin (BSA)] to remove saponin.

Determination of mitochondrial respiratory rates

Mitochondrial respiratory rates were measured by polarographic oxygen sensors in a two-chamber Oxygraph (OROBOROS® Instruments, Innsbruck, Austria) equipped with a Peltier thermostat and electromagnetic stirrers. All measurements were performed in triplicates. The oxygen concentration was recorded using the acquisition software DatLab (OROBOROS Instruments) and oxygen consumption rates (pmol O_2/s) were calculated and expressed as specific oxygen consumption rates (pmol O_2/s/unit CS). Measurements were performed using 10–15 µl of isolated mitochondria (10–18 mg mitochondrial protein/ml) in 2.2 ml of respiration buffer 1 (0.5 mM EGTA, 3 mM $MgCl_2$, 20 mM taurine, 10 mM KH_2PO_4, 20 mM HEPES, 200 mM sucrose, 0.1% BSA, final pH 7.1) at 30°C, with continuous stirring. Two different substrate-inhibitor titration regimens were applied: in the first, respiration was stimulated by glutamate/malate (10/5 mM) and ADP (2 mM). After inhibition by antimycin A (5 µM), complex IV respiration was directly measured by the addition of TMPD/ascorbate (200 µM/2 mM). First, respiration was uncoupled by full permeabilization with FCCP (1.5 µM). Secondly, respiration was stimulated by pyruvate/malate (10/5 mM) and ADP (2 mM) (state 3 respiration), followed by the inhibition of the ATP–ADP translocase by atractyloside (50 µM) to determine the rate of uncoupled (state 4) respiration.

For the analysis of the permeabilized muscle fibres of the soleus muscle, fibres were incubated in 2.2 ml respiration buffer 2 at 30°C under continuous stirring. After the addition of palmitoyl carnitine/malate (500 µM/5 mM), ADP (2 mM) was added and the oxygen consumption rate was determined.

Determination of CS, NADH:O_2 oxidoreductase, succinate:cytochrome *c* oxidoreductase and cytochrome *c* oxidase activities

In mitochondrial preparations that had been frozen and thawed once, we measured the activities of the respiratory chain enzymes NADH:O_2 oxidoreductase (complex I/III/IV), succinate:cytochrome *c* oxidoreductase (complex II/III), cytochrome *c* oxidase (complex IV) and CS activity as marker enzyme for mitochondrial activity, to which the other activities were normalized.

CS activity was monitored by following the reduction of 5,5′-dithiobis-(2-nitrobenzoic) acid (DTNB) at 412 nm (Hitachi U-3010 spectrophotometer) at 37°C after full permeabilization of mitochondria with 0.5% Triton X-100. Briefly, 750 µl H_2O, 100 µl DTNB (0.4 mg/ml in 1 M Tris–Cl, pH 8) and 30 µl acetyl-coenzyme A (10 mg/ml in H_2O) were pre-incubated with 100 µl of permeabilized mitochondria, and the reaction subsequently started by the addition of 20 µl oxalacetic acid (3.3 mg/ml in 50 mM Tris–Cl, pH 7.5). A molar extinction coefficient of 13 600/mol/cm was used to calculate the amount of CS activity.

The rotenone-sensitive NADH:O_2 oxidoreductase activity was determined as previously described (37). Briefly, 720 µl

of a test mixture containing 50 mM K_3PO_4, 2.5 mg/ml BSA, 0.2 mM NADH, 5 mM $MgCl_2$, 130 μg/ml cytochrome *c*, pH 7.4 were pre-incubated at 30°C for 5 min; the reaction was started by adding 30 μl of the mitochondrial preparation. After 4 min of measurement, rotenone was added to 8 μg/ml.

Complex II and III activity was determined by measuring succinate:cytochrome *c* oxidoreductase activity (38). After pre-incubation of 920 μl test mixture (20 mM K_3PO_4, pH 7.5, 2 mM EDTA, 2 mM NaN_3, 1.8 mg/ml oxidized cytochrome *c*, 1.3 mM succinate, 4 μg/ml rotenone) for 5 min at 30°C, 40 μl of the mitochondrial preparation were added to start the reaction.

The activity of cytochrome *c* oxidase (complex IV) was measured by following the oxidation of reduced cytochrome *c* at 550 nm. Briefly, 980 μl of 0.09 mM cytochrome *c* (prepared by reduction using sodium dithionite and subsequent removal of dithionite with N_2) in 100 mM HEPES (pH 7.2) were pre-incubated for 10 min at 30°C, and the reaction started by the addition of 40 μl of the mitochondrial preparation. After 8 min of measurement cytochrome *c* was completely oxidized by the addition of K_3 (Fe $(CN)_6$) to determine the amount of oxidizeable cytochrome *c*. For the calculation of enzyme activity, a molar extinction coefficient of 21 100/mol/cm was used.

β-Oxidation

The rate of β-oxidation in semi-permeabilized mitochondria and peroxisomes (isolated from mouse skeletal muscle) and in cultured fibroblasts was determined in duplicate as described elsewhere (39). Briefly, in separate reactions, $1-2 \times 10^5$ d.p.m. of [1-^{14}C]lignoceric acid (C24:0) and [1-^{14}C]palmitic acid (C16:0) obtained from American Radiolabelled Chemicals (St Louis, MO, USA) were brought to 5 nmol with the respective unlabelled fatty acid and added to the fibroblasts, mitochondria and peroxisomes. After 1 h of incubation at 37°C, the amount of degraded fatty acids was determined by measuring the release of water-soluble radioactivity. The β-oxidation activity was calculated as nanomole water-soluble ^{14}C/h/mg protein and the C24:0/C16:0 ratio was determined.

Analysis of VLCFA content by gas chromatography and electrospray ionization mass spectrometry

For analysis of the level of VLCFA in skeletal muscle, gastrocnemius, quadriceps, soleus and adductors muscles were dissected from the hind limbs and pooled for each of three *Abcd1*-deficient and three wild-type control mice sacrificed at the age of 9 months. Gas chromatographic analysis was performed as described previously (8). Fatty acid content of isolated mitochondria (as described earlier) was analysed by electrospray ionization mass spectrometry as described recently (40).

Ultrastructural analysis of the diaphragm

Small stripes of diaphragm from wild-type and *Abcd1*-deficient mice were immersed in Karnovsky fixative (4% paraformaldehyde, 5% glutaraldehyde), post-fixed in osmium tetroxide and finally embedded in epoxy resin. Ultrathin sections were stained with uranyl acetate/lead citrate and viewed using a transmission electron microscope (Jeol 1200EX II, Jeol, Japan). Morphometric parameters of muscle mitochondria were collected from digitalized photomicrographs, using Image-J software (http://rsb.info.nih.gov/ij/).

Measurement of ATP synthesis in permeabilized human fibroblasts

ATP synthesis was measured in selectively permeabilized human primary fibroblasts derived from X-ALD patients and healthy controls following the procedure described by Wanders *et al.* (24). In short, cultured fibroblasts were incubated at a final concentration of 0.2 mg/ml in a medium containing 150 mM KCl, 25 mM Tris–Cl (pH 7.4), 2 mM EDTA, 10 mM potassium phosphate, 1 mM ADP, 0.1% (w/v) BSA, 40 μg/ml digitonin plus a respiratory substrate. Reactions were allowed to proceed for 30 min followed by the termination of reactions by perchloric acid. In the neutralized protein-free, perchloric acid extracts, ATP was measured spectrophotometrically (24).

Lactate and pyruvate formation from glucose in human fibroblasts

The clinical presentation of patients with mitochondrial dysfunction due to respiratory chain defects is very heterogeneous. One biochemical parameter that is determined is the lactate to pyruvate ratio, which increases caused by a shift in the cytosolic redox state due to the impaired NADH oxidation via the respiratory chain. For experimental design refer Wijburg *et al.* (25).

Statistical analysis

P-values were calculated by using the two-tailed Student's *t*-test. *P*-values <0.05 were used as criteria for statistical significance.

ACKNOWLEDGEMENTS

We thank Mihaela Žigmann, Martina Krammer, Thomas Korosec, Regina Wegscheider, Jos Ruiter and Fredoen Valianpour for excellent technical assistance. This work was supported by the Austrian National Bank (Grant 9043), the European Leukodystrophy Association (ELA, Nancy, France) and the European Union Project LSHM-CT-2004-502987.

REFERENCES

1. Aubourg, P. (ed.) (1996) *X-linked Adrenoleukodystrophy.* Elsevier, Amsterdam.
2. Moser, H.W., Smith, K.D., Watkins, P.A., Powers, J., Moser, A.B. (2001) *X-linked Adrenoleukodystrophy.* McGrawHill, New York.
3. Mosser, J., Douar, A.M., Sarde, C.O., Kioschis, P., Feil, R., Moser, H., Poustka, A.M., Mandel, J.L. and Aubourg, P. (1993) Putative X-linked adrenoleukodystrophy gene shares unexpected homology with ABC transporters. *Nature*, **361**, 726–730.

4. Holzinger, A., Kammerer, S., Berger, J. and Roscher, A.A. (1997) cDNA cloning and mRNA expression of the human adrenoleukodystrophy related protein (ALDRP), a peroxisomal ABC transporter. *Biochem. Biophys. Res. Commun.*, **239**, 261–264.
5. Kamijo, K., Kamijo, T., Ueno, I., Osumi, T. and Hashimoto, T. (1992) Nucleotide sequence of the human 70 kDa peroxisomal membrane protein: a member of ATP-binding cassette transporters. *Biochim. Biophys. Acta*, **1129**, 323–327.
6. Shani, N., Jimenez-Sanchez, G., Steel, G., Dean, M. and Valle, D. (1997) Identification of a fourth half ABC transporter in the human peroxisomal membrane. *Hum. Mol. Genet.*, **6**, 1925–1931.
7. Holzinger, A., Kammerer, S. and Roscher, A.A. (1997) Primary structure of human PMP69, a putative peroxisomal ABC-transporter. *Biochem. Biophys. Res. Commun.*, **237**, 152–157.
8. Forss-Petter, S., Werner, H., Berger, J., Lassmann, H., Molzer, B., Schwab, M.H., Bernheimer, H., Zimmermann, F. and Nave, K.A. (1997) Targeted inactivation of the X-linked adrenoleukodystrophy gene in mice. *J. Neurosci. Res.*, **50**, 829–843.
9. Kobayashi, T., Shinnoh, N., Kondo, A. and Yamada, T. (1997) Adrenoleukodystrophy protein-deficient mice represent abnormality of very long chain fatty acid metabolism. *Biochem. Biophys. Res. Commun.*, **232**, 631–636.
10. Lu, J.F., Lawler, A.M., Watkins, P.A., Powers, J.M., Moser, A.B., Moser, H.W. and Smith, K.D. (1997) A mouse model for X-linked adrenoleukodystrophy. *Proc. Natl Acad. Sci. USA*, **94**, 9366–9371.
11. Pujol, A., Hindelang, C., Callizot, N., Bartsch, U., Schachner, M. and Mandel, J.L. (2002) Late onset neurological phenotype of the X-ALD gene inactivation in mice: a mouse model for adrenomyeloneuropathy. *Hum. Mol. Genet.*, **11**, 499–505.
12. Wanders, R.J., van Roermund, C.W., van Wijland, M.J., Schutgens, R.B., van den Bosch, H., Schram, A.W. and Tager, J.M. (1988) Direct demonstration that the deficient oxidation of very long chain fatty acids in X-linked adrenoleukodystrophy is due to an impaired ability of peroxisomes to activate very long chain fatty acids. *Biochem. Biophys. Res. Commun.*, **153**, 618–624.
13. Lazo, O., Contreras, M., Hashmi, M., Stanley, W., Irazu, C. and Singh, I. (1988) Peroxisomal lignoceroyl-CoA ligase deficiency in childhood adrenoleukodystrophy and adrenomyeloneuropathy. *Proc. Natl Acad. Sci. USA*, **85**, 7647–7651.
14. Wanders, R.J., van Roermund, C.W., van Wijland, M.J., Nijenhuis, A.A., Tromp, A., Schutgens, R.B., Brouwer-Kelder, E.M., Schram, A.W., Tager, J.M., van den Bosch, H. *et al.* (1987) X-linked adrenoleukodystrophy: defective peroxisomal oxidation of very long chain fatty acids but not of very long chain fatty acyl-CoA esters. *Clin. Chim. Acta*, **165**, 321–329.
15. Hashmi, M., Stanley, W. and Singh, I. (1986) Lignoceroyl-CoASH ligase: enzyme defect in fatty acid beta-oxidation system in X-linked childhood adrenoleukodystrophy. *FEBS Lett.*, **196**, 247–250.
16. McGuinness, M.C., Lu, J.F., Zhang, H.P., Dong, G.X., Heinzer, A.K., Watkins, P.A., Powers, J. and Smith, K.D. (2003) Role of ALDP (ABCD1) and mitochondria in X-linked adrenoleukodystrophy. *Mol. Cell Biol.*, **23**, 744–753.
17. Heinzer, A.K., Watkins, P.A., Lu, J.F., Kemp, S., Moser, A.B., Li, Y.Y., Mihalik, S., Powers, J.M. and Smith, K.D. (2003) A very long-chain acyl-CoA synthetase-deficient mouse and its relevance to X-linked adrenoleukodystrophy. *Hum. Mol. Genet.*, **12**, 1145–1154.
18. Steinberg, S.J., Kemp, S., Braiterman, L.T. and Watkins, P.A. (1999) Role of very-long-chain acyl-coenzyme A synthetase in X-linked adrenoleukodystrophy. *Ann. Neurol.*, **46**, 409–412.
19. Dammai, V. and Subramani, S. (2001) The human peroxisomal targeting signal receptor, Pex5p, is translocated into the peroxisomal matrix and recycled to the cytosol. *Cell*, **105**, 187–196.
20. Gould, S.J. and Valle, D. (2000) Peroxisome biogenesis disorders: genetics and cell biology. *Trends Genet.*, **16**, 340–345.
21. Baes, M., Gressens, P., Baumgart, E., Carmeliet, P., Casteels, M., Fransen, M., Evrard, P., Fahimi, D., Declercq, P.E., Collen, D. *et al.* (1997) A mouse model for Zellweger syndrome. *Nat. Genet.*, **17**, 49–57.
22. Baumgart, E., Vanhorebeek, I., Grabenbauer, M., Borgers, M., Declercq, P.E., Fahimi, H.D. and Baes, M. (2001) Mitochondrial alterations caused by defective peroxisomal biogenesis in a mouse model for Zellweger syndrome (PEX5 knockout mouse). *Am. J. Pathol.*, **159**, 1477–1494.
23. Theda, C., Moser, A.B., Powers, J.M. and Moser, H.W. (1992) Phospholipids in X-linked adrenoleukodystrophy white matter: fatty acid abnormalities before the onset of demyelination. *J. Neurol. Sci.*, **110**, 195–204.
24. Wanders, R.J., Ruiter, J.P. and Wijburg, F.A. (1993) Studies on mitochondrial oxidative phosphorylation in permeabilized human skin fibroblasts: application to mitochondrial encephalomyopathies. *Biochim. Biophys. Acta*, **1181**, 219–222.
25. Wijburg, F.A., Feller, N., Scholte, H.R., Przyrembel, H. and Wanders, R.J. (1989) Studies on the formation of lactate and pyruvate from glucose in cultured skin fibroblasts: implications for detection of respiratory chain defects. *Biochem. Int.*, **19**, 563–570.
26. Molzer, B., Bernheimer, H., Budka, H., Pilz, P. and Toifl, K. (1981) Accumulation of very long chain fatty acids is common to 3 variants of adrenoleukodystrophy (ALD). 'Classical' ALD, atypical ALD (female patient) and adrenomyeloneuropathy. *J. Neurol. Sci.*, **51**, 301–310.
27. Moser, H.W., Moser, A.B., Kawamura, N., Murphy, J., Suzuki, K., Schaumburg, H. and Kishimoto, Y. (1980) Adrenoleukodystrophy: elevated C26 fatty acid in cultured skin fibroblasts. *Ann. Neurol.*, **7**, 542–549.
28. Moser, H.W., Moser, A.B., Frayer, K.K., Chen, W., Schulman, J.D., O'Neill, B.P. and Kishimoto, Y. (1981) Adrenoleukodystrophy: increased plasma content of saturated very long chain fatty acids. *Neurology*, **31**, 1241–1249.
29. Askanas, V., McLaughlin, J., Engel, W.K. and Adornato, B.T. (1979) Abnormalities in cultured muscle and peripheral nerve of a patient with adrenomyeloneuropathy. *N. Engl. J. Med.*, **301**, 588–590.
30. Hughes, J.L., Poulos, A., Robertson, E., Chow, C.W., Sheffield, L.J., Christodoulou, J. and Carter, R.F. (1990) Pathology of hepatic peroxisomes and mitochondria in patients with peroxisomal disorders. *Virchows Arch. A Pathol. Anat. Histopathol.*, **416**, 255–264.
31. Gnaiger, E., Steinlechner-Maran, R., Mendez, G., Eberl, T. and Margreiter, R. (1995) Control of mitochondrial and cellular respiration by oxygen. *J. Bioenerg. Biomembr.*, **27**, 583–596.
32. Kuznetsov, A.V., Strobl, D., Ruttmann, E., Konigsrainer, A., Margreiter, R. and Gnaiger, E. (2002) Evaluation of mitochondrial respiratory function in small biopsies of liver. *Anal. Biochem.*, **305**, 186–194.
33. Kemp, S., Wei, H.M., Lu, J.F., Braiterman, L.T., McGuinness, M.C., Moser, A.B., Watkins, P.A. and Smith, K.D. (1998) Gene redundancy and pharmacological gene therapy: implications for X-linked adrenoleukodystrophy. *Nat. Med.*, **4**, 1261–1268.
34. Berger, J., Albet, S., Bentejac, M., Netik, A., Holzinger, A., Roscher, A.A., Bugaut, M. and Forss-Petter, S. (1999) The four murine peroxisomal ABC-transporter genes differ in constitutive, inducible and developmental expression. *Eur. J. Biochem.*, **265**, 719–727.
35. Schonfeld, P., Kahlert, S. and Reiser, G. (2004) In brain mitochondria the branched chain fatty acid phytanic acid impairs energy transduction and sensitizes for permeability transition. *Biochem. J.*, **383**, 121–128.
36. Kemp, S., Valianpour, F., Denis, S., Ofman, R., Sanders, R.J., Mooyer, P., Barth, P.G. and Wanders, R.J. (2005) Elongation of very long-chain fatty acids is enhanced in X-linked adrenoleukodystrophy. *Mol. Genet. Metab.*, **84**, 144–151.
37. Fischer, J.C., Ruitenbeek, W., Trijbels, J.M., Veerkamp, J.H., Stadhouders, A.M., Sengers, R.C. and Janssen, A.J. (1986) Estimation of NADH oxidation in human skeletal muscle mitochondria. *Clin. Chim. Acta*, **155**, 263–273.
38. Fischer, J.C., Ruitenbeek, W., Berden, J.A., Trijbels, J.M., Veerkamp, J.H., Stadhouders, A.M., Sengers, R.C. and Janssen, A.J. (1985) Differential investigation of the capacity of succinate oxidation in human skeletal muscle. *Clin. Chim. Acta*, **153**, 23–36.
39. Watkins, P.A., Ferrell, E.V., Jr, Pedersen, J.I. and Hoefler, G. (1991) Peroxisomal fatty acid beta-oxidation in HepG2 cells. *Arch. Biochem. Biophys.*, **289**, 329–336.
40. Valianpour, F., Selhorst, J.J., van Lint, L.E., van Gennip, A.H., Wanders, R.J. and Kemp, S. (2003) Analysis of very long-chain fatty acids using electrospray ionization mass spectrometry. *Mol. Genet. Metab.*, **79**, 189–196.